UE Géoressources — Partie 7 - R. Thiéry - 2026

Ressources métalliques et gisements

Résumé

Cette partie présente les processus de concentration des métaux, les grands types de gisements, les méthodes d'exploration et de traitement ainsi que les notions de criticité et d'impact minier.

Mots-clés

minerai • teneur • métallogénie • gisement • terres rares • exploration • traitement • drainage minier acide

Plan de la partie

CM 9	**Métaux, métallogénie et grands types de gisements** Métaux majeurs, métaux de base, métaux précieux et métaux critiques • Minerai, minéral utile, gangue, teneur et facteur de concentration • Teneur de coupure et notion économique de gisement • Affinités géochimiques et mobilité des éléments métalliques • Principes de concentration magmatique, hydrothermale, sédimentaire et supergène • Gisements magmatiques : Bushveld, Sudbury et Norilsk-Talnakh • Gisements de sulfures massifs volcanogènes • Porphyres cuprifères et systèmes hydrothermaux associés • Gisements de type MVT • Formations de fer rubané • Altération latéritique, bauxites et minerais de nickel • Placers et concentration mécanique • Terres rares : particularités géochimiques et principaux types de gisements • Pierres gemmes : diamant, rubis et saphir • Exploration minière : géologie, géochimie et géophysique • Ressources, réserves, criticité et sécurité d'approvisionnement	**Jeudi 12 novembre** 9h30-11h00 · B007
TD 7	**Terres rares : géochimie et étude de gisement** Propriétés chimiques des terres rares et contraction des lanthanides • Classification des terres rares légères et lourdes • Lecture et normalisation d'un spectre de terres rares • Interprétation d'anomalies en europium et en cérium • Comparaison de plusieurs roches ou minerais à partir de données analytiques • Étude d'un gisement de terres rares • Calcul de teneur et de quantité de métal contenue • Ressources, réserves et facteurs de récupération • QCM sur métaux critiques et terres rares	**Mercredi 25 novembre** 13h00-14h30 · B119
TD 8	**Exploitation minière, traitement des minerais et impacts** Calcul de tonnage, teneur moyenne et métal contenu • Teneur de coupure et distinction ressource / réserve • Exploitation à ciel ouvert et exploitation souterraine • Principes de fragmentation, broyage et concentration du minerai • Séparation gravimétrique, flottation et procédés métallurgiques : aperçu • Rendement de récupération et bilan matière d'une chaîne de traitement • Stériles miniers, résidus et parcs à résidus • Drainage minier acide : mécanismes et prévention • Pollution métallique : exemple du plomb • Réhabilitation des sites miniers • Recyclage, économie circulaire et réduction de la demande primaire	**Mercredi 2 décembre** 13h00-14h30 · B003

Fig. 1

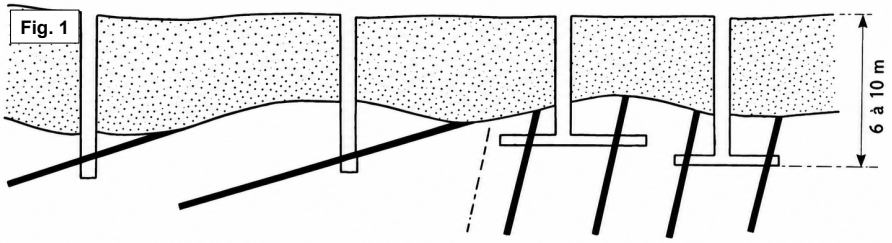

Fig. 103. Découvrement de la coupe par des fouilles lors d'un faible pendage et par des fouilles avec travers-banc lors d'un fort pendage

Fig. 2

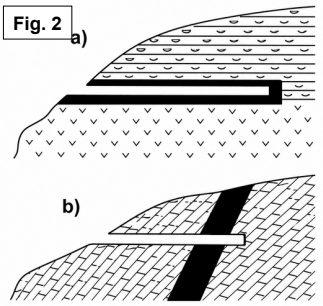

Fig. 105. Galeries :
a — longitudinale ; *b* — transversale

Fig. 3

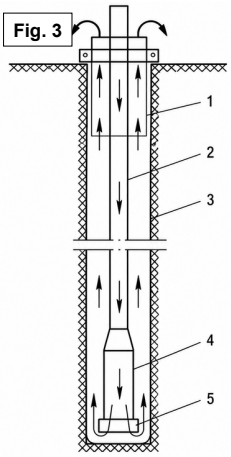

Fig. 110. Schéma du lavage des trous :
1 — tube de cuvelage ; 2 — tube de forage ; 3 — paroi du trou ; 4 — tube carottier ; 5 — couronne

Fig. 4

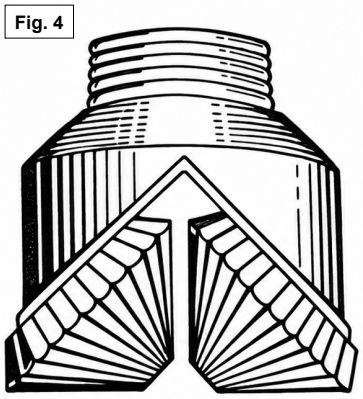

Fig. 107. Burin à fraise

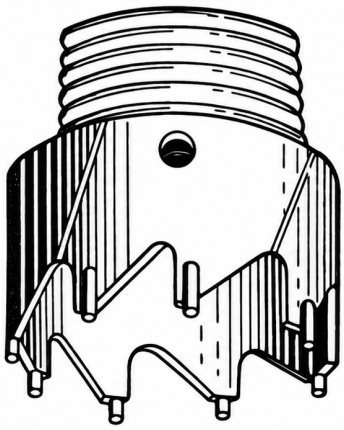

Fig. 108. Couronne annulaire (à pobédite)

Fig. 5

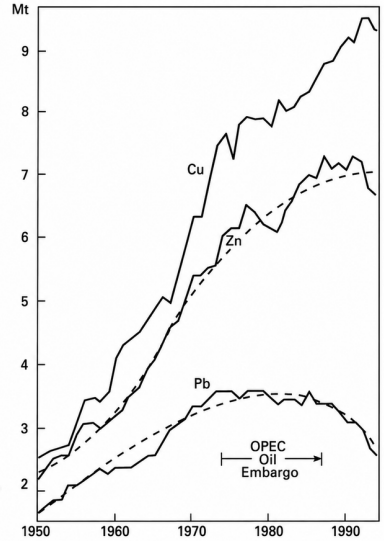

Fig. 2.3 World production of copper, zinc and lead from 1950 to 1994. General trends for zinc and lead superimposed.

Fig. 6

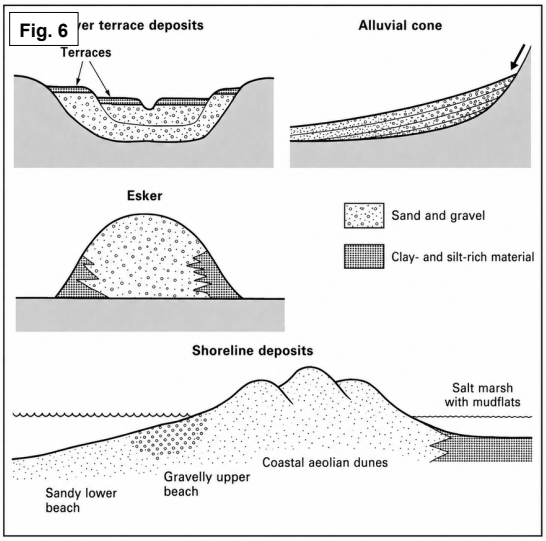

Fig. 21.1 Sketch sections (at different scales) of selected types of sand and gravel deposits.

Fig. 7

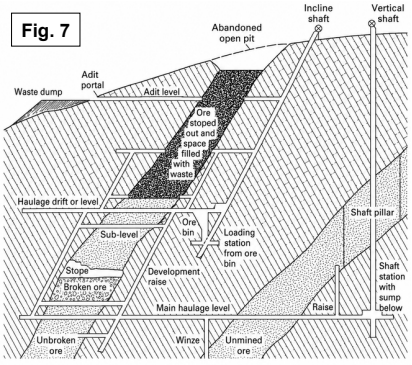

Fig. 2.9 Mining terminology. *Ore was first mined at the outcrop from an open pit; then an adit was driven into the hillside to intersect and mine the ore at a lower level. An inclined shaft was sunk later to mine at even deeper levels and, eventually, a vertical shaft was sunk to serve operations to two orebodies more efficiently. Ore is mined by driving two haulage drifts at different levels and connecting them by raises which are then connected by sublevels. Ore is mined upwards from the lower sublevel to form a stope. Broken ore can be left in the stope to form a working platform and to support its walls (shrinkage stoping), or withdrawn and waste from the mill pumped in (cut-and-fill stoping). Ore between haulage and sublevel is left as supporting pillars until the level is abandoned. A shaft pillar is also left unmined. (After Barnes, 1988, Ores and Minerals, Open University Press, with permission.)*

Fig. 8

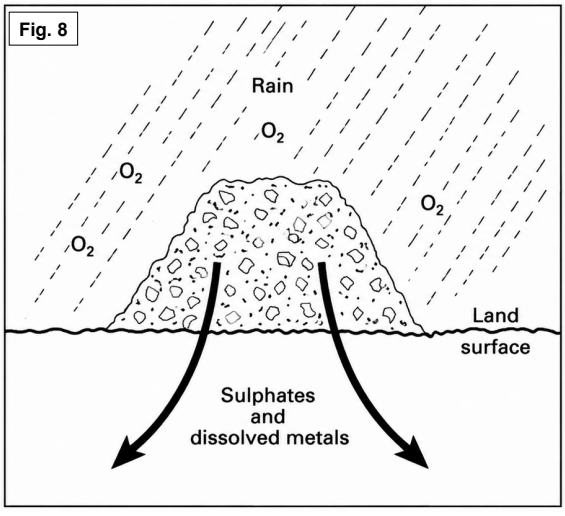

Fig. 3.1 Generation of polluting acid water by oxidizing rain water percolating through a waste heap containing sulphides.

Fig. 9

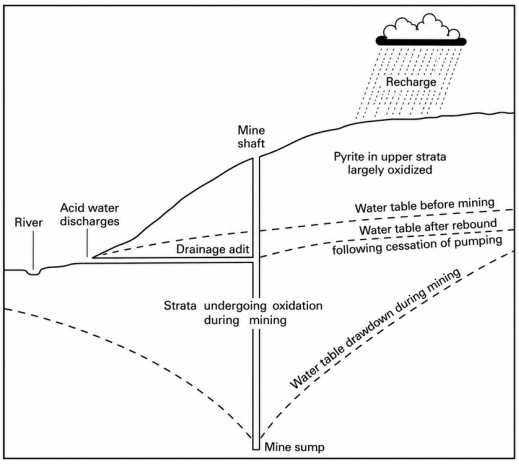

Fig. 3.2 Generation of acid water during mine dewatering followed by closure. During mining, drainage through the adit from strata above adit level and water pumped into it from lower levels produces an acid flow into the neighbouring river. After mine closure, water table rebound produces an initial, large outflush of concentrated acid water with high metal content through the adit and/or surrounding surface strata into the surface drainage, followed by a continuing lower volume, but still highly polluting, outflow.

Fig. 10

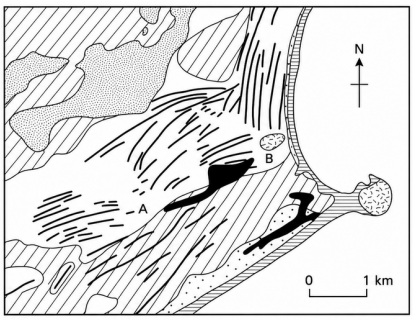

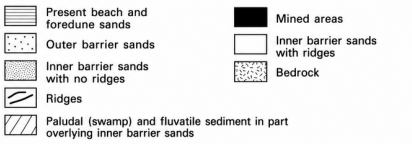

Fig. 4.8 Geology and mining areas of the beach sand deposits of Crowdy Head, New South Wales.

Fig. 11

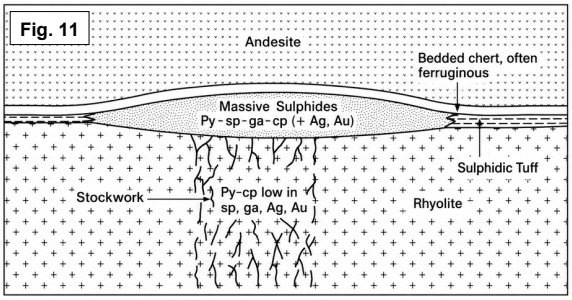

Fig. 4.10 Schematic cross section through an idealized volcanic-associated massive sulphide deposit showing the underlying feeder stockwork and typical mineralogy. Py, pyrite; sp, sphalerite; ga, galena; cp, chalcopyrite.

Fig. 12

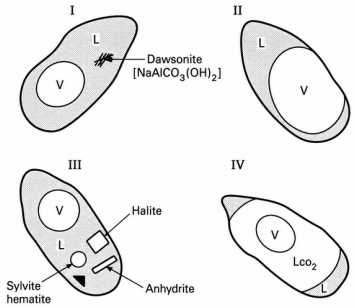

Fig. 5.3 Sketches of four important types of fluid inclusions. L, aqueous fluid; V, vapour; Lco_2, liquid CO_2. For explanation see text.

Fig. 13

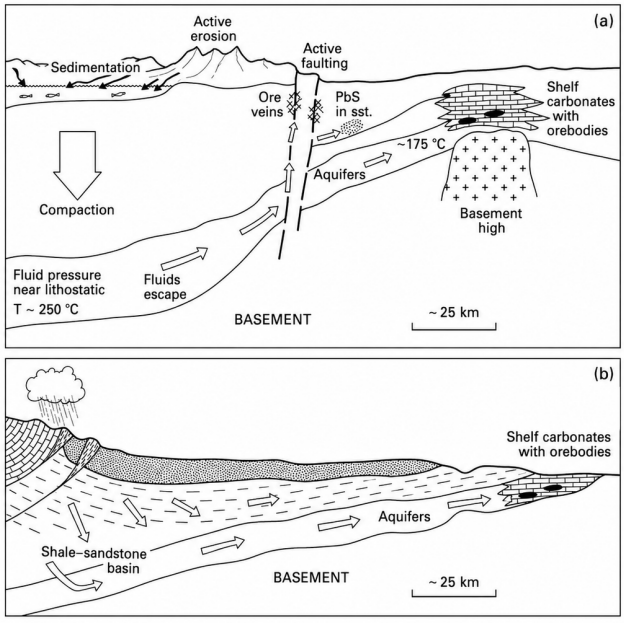

Fig. 6.3 Schemata for the formation of Mississippi Valley-type deposits. (a) Overpressured, hot pore fluids escape from a shale basin (perhaps aided by hydraulic fracturing) and move up aquifers to form deposits in cooler strata, filling fractures or forming other types of orebody. (b) Gravity-driven fluids flowing from a hydraulic head in a highland area flush through a basin driving out and replenishing the formation waters.

Fig. 14

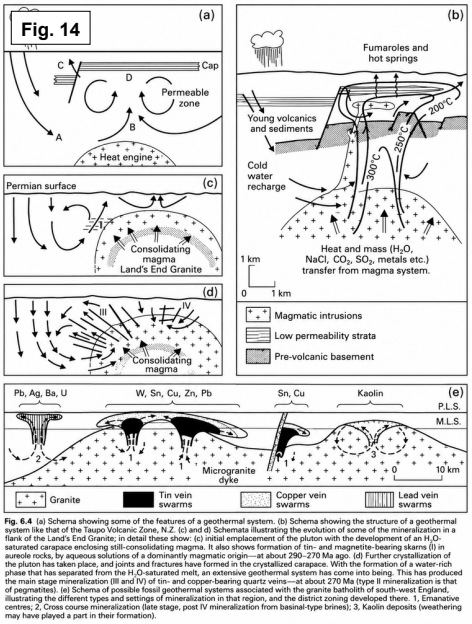

Fig. 6.4 (a) Schema showing some of the features of a geothermal system. (b) Schema showing the structure of a geothermal system like that of the Taupo Volcanic Zone, N.Z. (c) and d) Schemata illustrating the evolution of some of the mineralization in a flank of the Land's End Granite; in detail these show: (c) initial emplacement of the pluton with the development of an H_2O-saturated carapace enclosing still-consolidating magma. It also shows formation of tin- and magnetite-bearing skarns (I) in aureole rocks, by aqueous solutions of a dominantly magmatic origin—at about 290–270 Ma ago. (d) Further crystallization of the pluton has taken place, and joints and fractures have formed in the crystallized carapace. With the formation of a water-rich phase that has separated from the H_2O-saturated melt, an extensive geothermal system has come into being. This has produced the main stage mineralization (III and IV) of tin- and copper-bearing quartz veins—at about 270 Ma (type II mineralization is that of pegmatites). (e) Schema of possible fossil geothermal systems associated with the granite batholith of south-west England, illustrating the different types and settings of mineralization in that region, and the district zoning developed there. 1, Emanative centres; 2, Cross course mineralization (late stage, post IV mineralization from basinal-type brines); 3, Kaolin deposits (weathering may have played a part in their formation).

Fig. 15

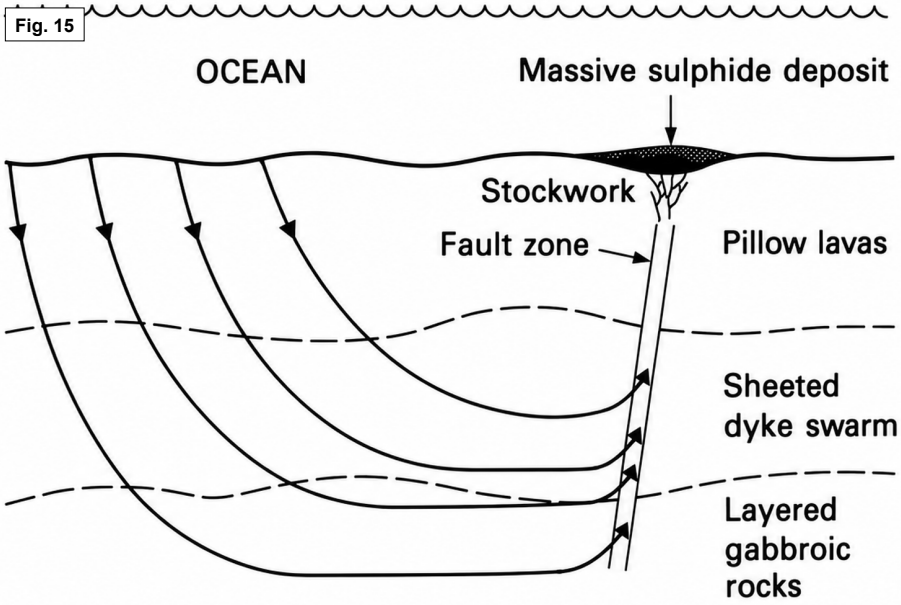

Fig. 6.7 Diagram showing how sea water circulation through oceanic crust might give rise to the formation of an exhalative volcanic-associated massive sulphide deposit.

Fig. 16

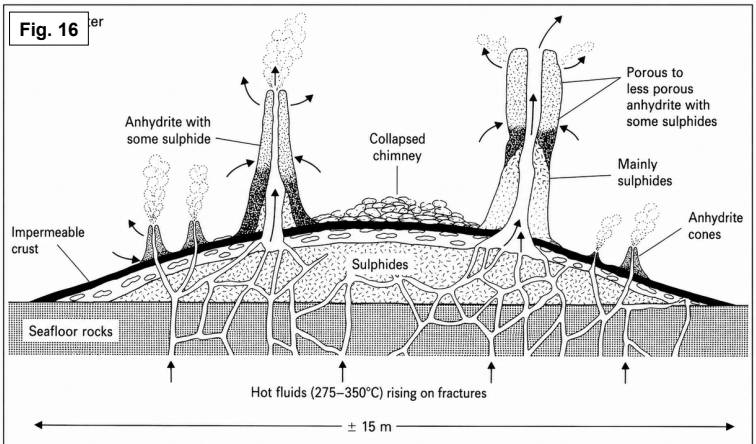

Fig. 6.8 Formation of chimneys and sulphide mounds on the sea floor. (After Barnes, 1988, *Ores and Minerals*, Open University Press, with permission.)

Fig. 17

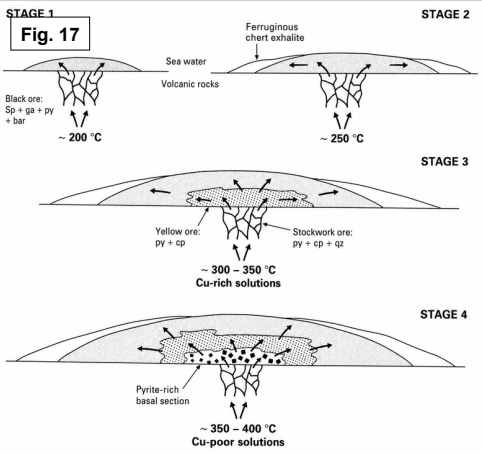

Fig. 6.9 Diagrams to illustrate the first four stages during the formation of volcanic-associated massive sulphide deposits as described in the text; bar = baryte, cp = chalcopyrite, ga = galena, py = pyrite, qz = quartz, and sp = sphalerite.

Fig. 18

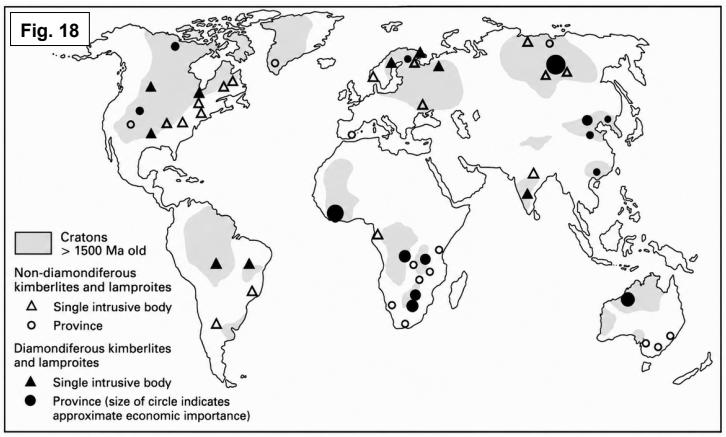

Fig. 9.1 Distribution of diamondiferous and non-diamondiferous kimberlites and lamproites.

Fig. 19

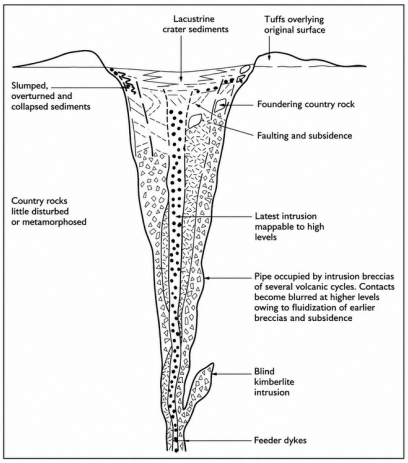

Fig. 9.3 Schematic diagram of a kimberlite diatreme (pipe) and maar (volcanic crater below ground level and surrounded by a low tuff rim). The maar can be up to 2 km across.

Fig. 20

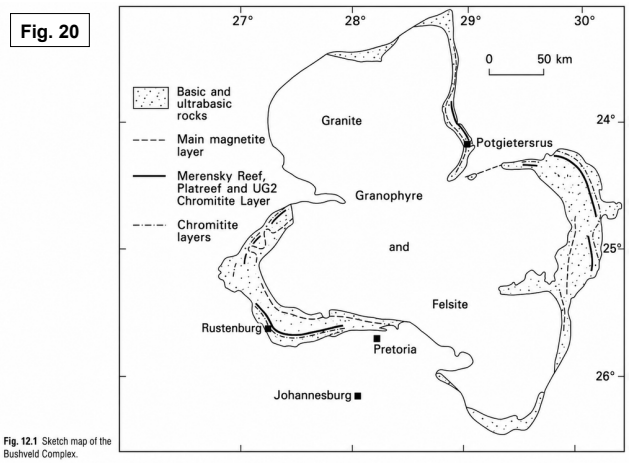

Fig. 12.1 Sketch map of the Bushveld Complex.

Fig. 21

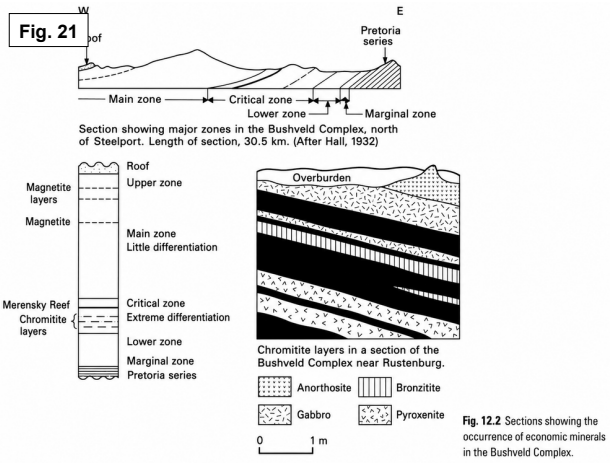

Fig. 12.2 Sections showing the occurrence of economic minerals in the Bushveld Complex.

Fig. 22

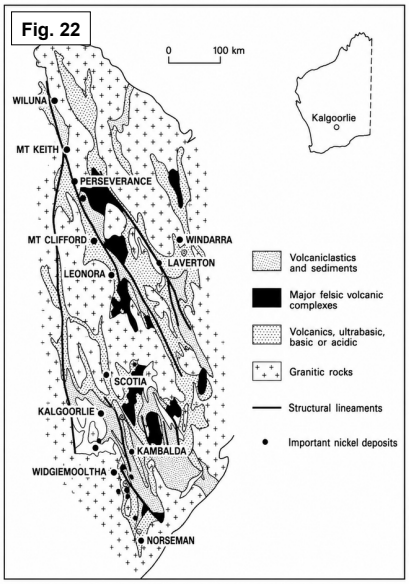

Fig. 13.3 Generalized geological map of the Eastern Goldfields Province of the Yilgarn Block showing some of the important nickel deposits.

Fig. 23

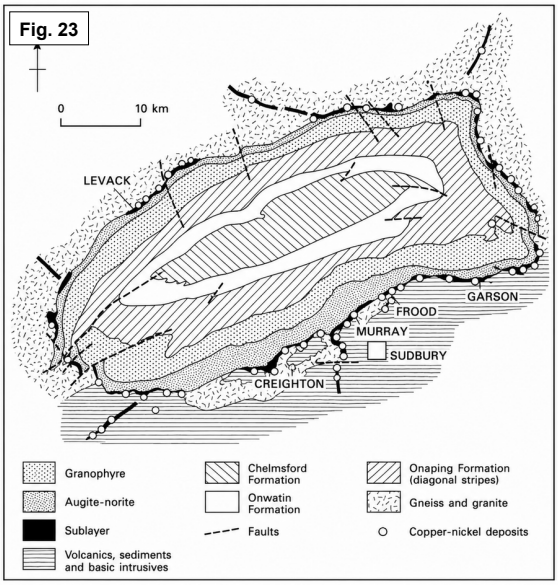

Fig. 13.5 Geological map of the Sudbury District.

Fig. 24

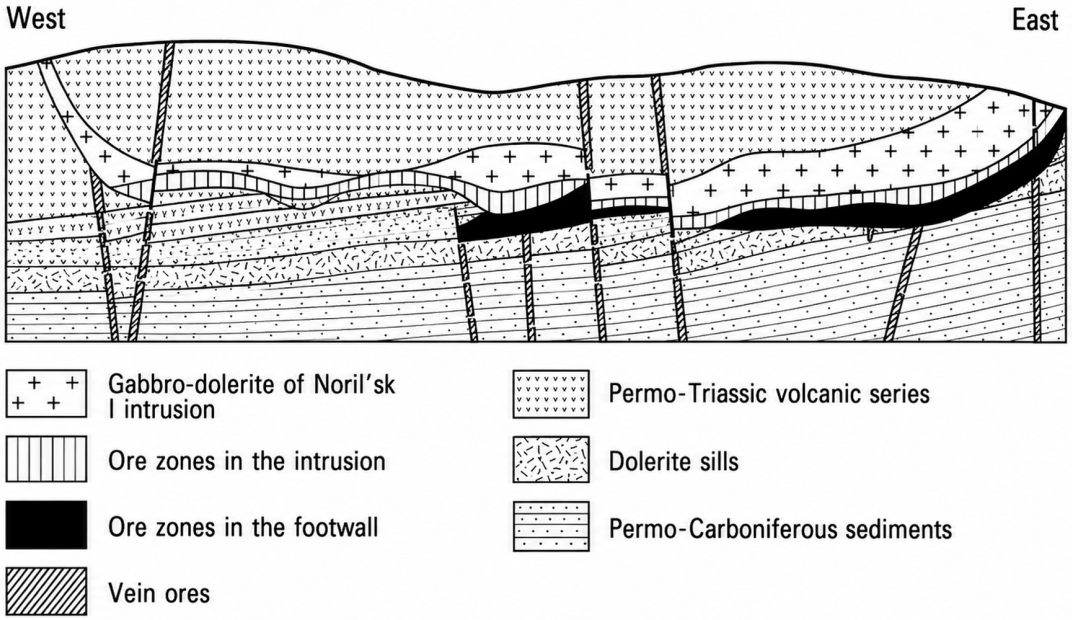

Fig. 13.8 Cross section through the Noril'sk I deposit.

Fig. 25

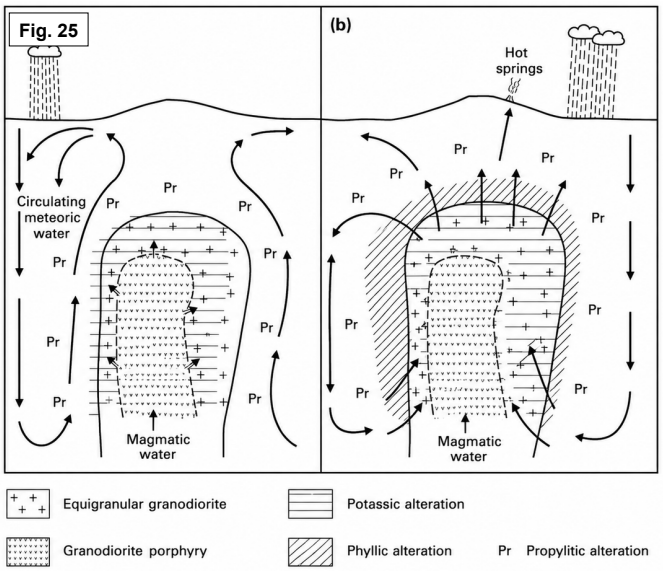

Fig. 15.7 Diagrammatic sections through a porphyry copper deposit showing two stages in the development of the hydrothermal fluids leading to the formation of a Lowell–Guilbert model deposit (b). Pr, propylitic alteration.

Fig. 26

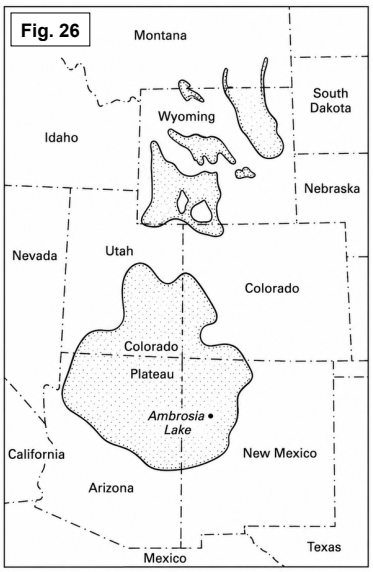

Fig. 18.3 Map showing the Colorado Plateau and Wyoming Basin.

Fig. 27

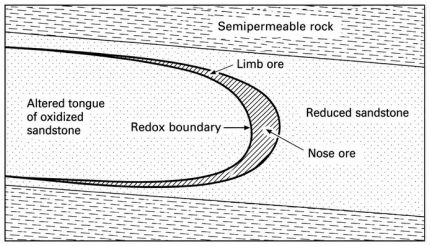

Fig. 18.4 Idealized cross section of a roll-front uranium deposit.

Fig. 28

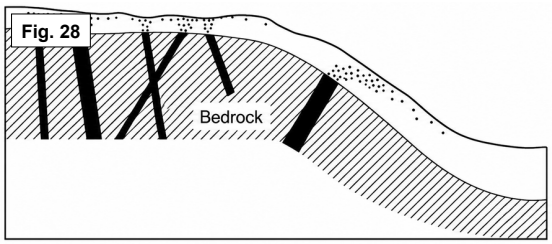

Fig. 19.1 The formation of residual (left) and eluvial (right) placer deposits by the weathering of cassiterite veins.

Fig. 29

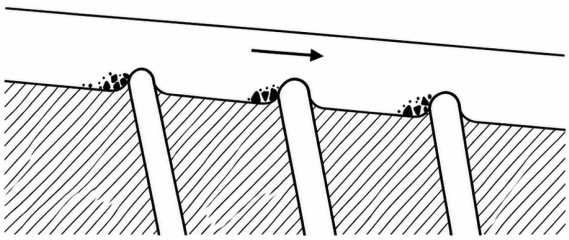

Fig. 19.2 Quartz ribs interbedded with slate serving as natural riffles for the collection of placer gold.

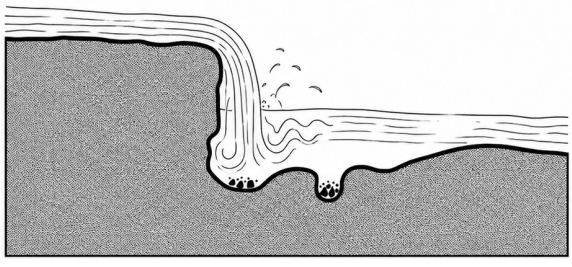

Fig. 19.3 Plunge pools at the foot of a waterfall and potholes can be sites of heavy mineral accumulations.

Fig. 30

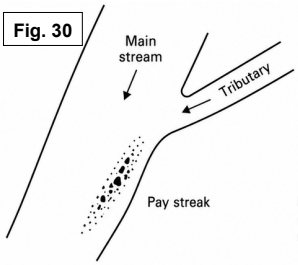

Fig. 19.4 A pay streak may be formed where a fast-flowing tributary enters a master stream.

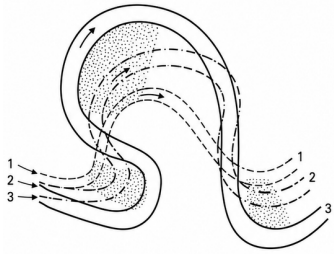

Fig. 19.5 Formation of pay streaks (dotted) in a rapidly flowing meandering stream with migrating meanders. 1, Original position of stream; 2, intermediate position; 3, present position. Note that pay streaks are extended laterally and downstream. Arrows indicate direction of water flow.

Fig. 31

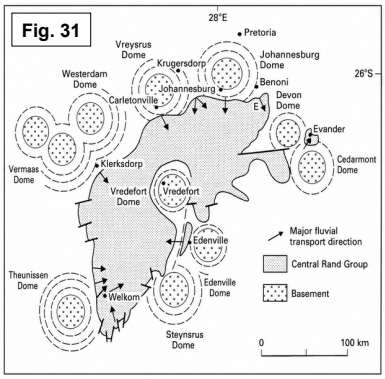

Fig. 19.9 Map showing the distribution of the Central Rand Group, which contains the principal Au–U mineralization within the Witwatersrand Goldfields, together with adjacent granite domes and sites of major fluvial influx. E indicates the position of the East Rand Goldfield (Fig. 4.9).

Fig. 32

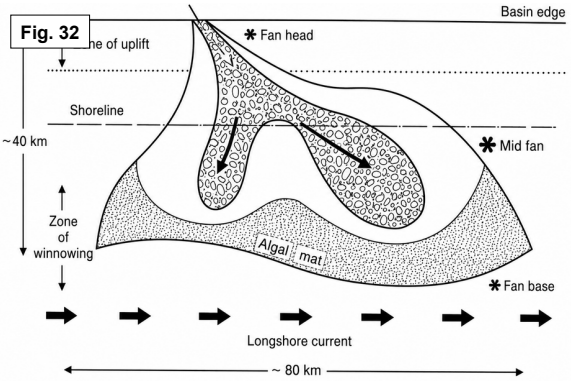

Fig. 19.10 Formation of a deltaic fan in the Witwatersrand Basin. The coarse material is shown by the pebble pattern, the algal mat by the finer pattern. Asterisk sizes indicate the relative gold values. (From Barnes, 1988, *Ores and Minerals*, Open University Press, with permission.)

Fig. 33

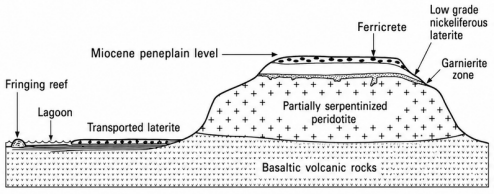

Fig. 20.1 Diagrammatic profile of a peridotite occurrence in New Caledonia showing the development of a residual nickel deposit.

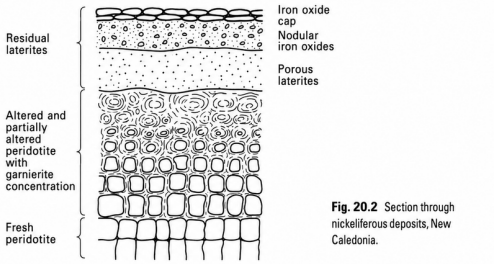

Fig. 20.2 Section through nickeliferous deposits, New Caledonia.

Fig. 34

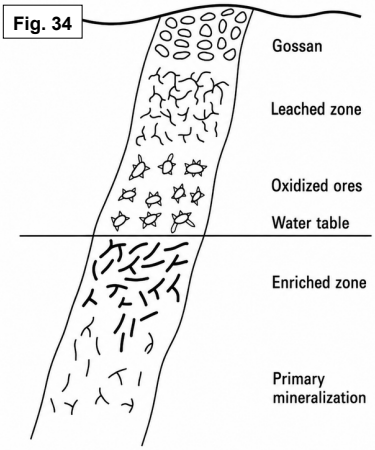

Fig. 20.3 Generalized section through a sulphide-bearing vein showing supergene enrichment.

Fig. 35

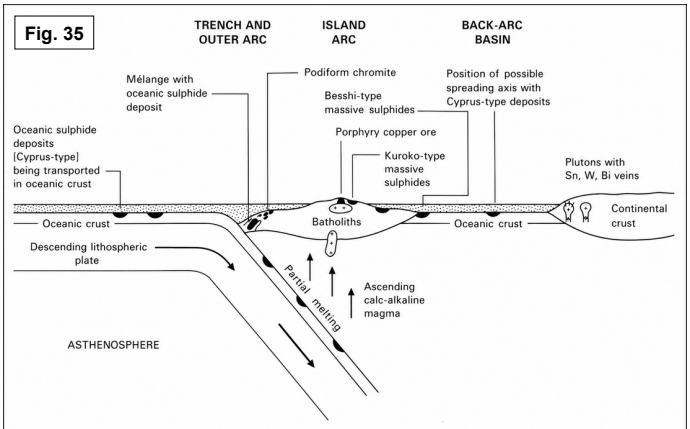

Fig. 29.7 Diagram showing the development and emplacement of some mineral deposits in an island arc and its adjacent regions.

Fig. 36

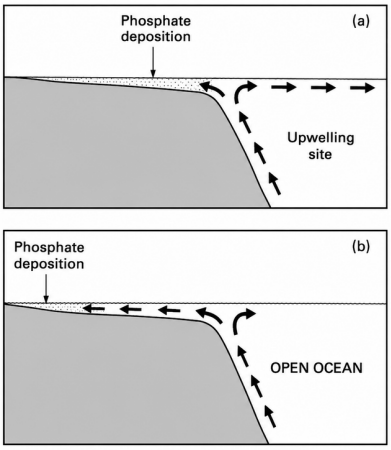

Fig. 21.3 Possible model for phosphorite formation beside an upwelling site initiated in a deep ocean. (a) Nutrient rich, deep ocean water floods on to the continental shelf and low grade phosphorite deposits form. (b) A sea level rise leads to a major marine transgression resulting in the reworking of phosphatic shelf sediments and the shoreward transport of phosphatic grains to form major deposits in the coastal zone and in marginal embayments.

Fig. 37

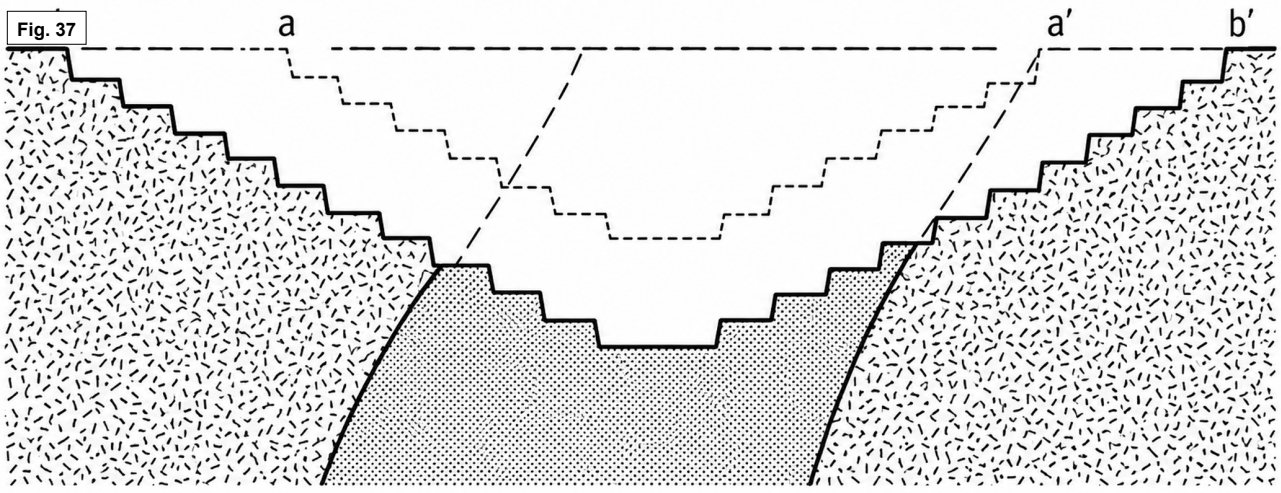

Fig. 2.8 Development of an open pit mine. During the early stages (a–a') more ore (black) is removed than waste rock; then, as the pit becomes deeper, the ratio of waste to ore mined becomes greater until at stage b–b' it is about 1.6 to 1. (After Barnes, 1988, *Ores and Minerals*, Open University Press, with permission.)